Reorganization Energy of Electron Transfer in Viscous Solvents above the Glass Transition

Pradip K. Ghorai and Dmitry V. Matyushov*

Department of Chemistry and Biochemistry and the Center for the Early Events in Photosynthesis, Arizona State University, P.O. Box 871604, Tempe, Arizona 85287-1604

Received: September 15, 2005; In Final Form: November 6, 2005

We present a molecular-dynamics study of the solvent reorganization energy of electron transfer in supercooled water. We observe a sharp decrease of the reorganization energy at a temperature identified as the temperature of structural arrest due to cage effect as discussed by the mode coupling theory. Both the heat capacity and dielectric susceptibility of the pure water show sharp drops at about the same temperature. This temperature also marks the onset of the enhancement of translational diffusion relative to rotational relaxation signaling the breakdown of the Stokes−Einstein relation. The change in the reorganization energy at the transition temperature reflects the dynamical arrest of the slow, collective relaxation of the solvent related to Debye relaxation of the solvent dipolar polarization.

I. Introduction

Theories of activated chemical dynamics and transport phenomena in a condensed phase are often based on transition-state ideas invoking equilibrium thermodynamics to describe the reaction flux across the transition-state surface separating the reactants from the products. The Marcus−Hush theory of electron transfer (ET) reactions fully relies on the transition-state formalism defining the ET activation barrier in terms of two thermodynamic parameters, the free energy gap and the nuclear reorganization energy. The former is the difference in free energies between the final and initial ET states, and the latter determines the curvature of two free energy parabolas.[1] When the donor−acceptor energy gap ΔE is chosen as the reaction coordinate, the activation energy of ET follows from the assumption that the stationary statistics of ΔE are Gaussian

$$\frac{E^{\mathrm{act}}}{k_{\mathrm{B}}T}=\frac{\langle\Delta E\rangle^2}{2\langle(\delta\Delta E)^2\rangle} \tag{1}$$

where angular brackets refer to an equilibrium average. This equation is normally brought to the standard Arrhenius form by introducing the classical reorganization energy λ_0

$$\lambda_0=\langle(\delta\Delta E)^2\rangle/2k_{\mathrm{B}}T \tag{2}$$

The transition-state description becomes inapplicable when the time of passage of the activation barrier is comparable to the relaxation time of the condensed medium (solvent). The population of the activated state becomes depleted, and one arrives at the friction-affected chemical kinetics described by Kramers theory[2] and its modifications.[3] For ET, this regime corresponds to solvent-controlled reactions when the preexponential factor of the rate is inversely proportional to a solvent relaxation time.[4] One can anticipate the next step in this hierarchy of relaxation times when the time of the reaction itself (not just the time of barrier passage) becomes comparable to the solvent relaxation time. Such conditions, which apply to ultrafast reactions in high-temperature solvents and to reactions in slowly relaxing viscous solvents, will result in the loss of ergodicity of the system and in the breakdown of the equilibrium description of the reaction activation barrier (in contrast to the alteration of the rate preexponent in the Kramers description).[5] A general theory of chemical rates at such conditions is still missing even though nonergodic behavior may apply to a broad class of reactions in supercooled liquids and in biopolymers.[6] The latter case is particularly relevant to the problem of nonergodic activation since the dynamics of biopolymers is characterized by a broad spectrum of relaxation times,[7,8] and for a given reaction rate, at least a subset of nuclear modes may become nonergodic.

Once the system loses ergodicity, the equilibrium average in eq 2 should be replaced with the time average over the observation time τ_{obs}, $\langle\ldots\rangle_{\mathrm{obs}}$. The actual property which affects the activation barrier in eq 1 is the second cumulant of the energy gap fluctuations depending on the observation time. We will, however, use the analogy with eq 2 to *define* the nonergodic reorganization energy

$$\lambda_{\mathrm{s}}=\langle(\delta\Delta E)^2\rangle_{\mathrm{obs}}/2k_{\mathrm{B}}T \tag{3}$$

In the nonergodic regime, the averages entering the activation barrier depend on the observation window dictated by the rate constant $k_{\mathrm{ET}}\propto\tau_{\mathrm{obs}}^{-1}$. The rate constant itself then needs to be calculated from a self-consistent equation[5]

$$k_{\mathrm{ET}}\propto\exp[-E^{\mathrm{act}}(k_{\mathrm{ET}})/k_{\mathrm{B}}T] \tag{4}$$

The key portion of this formalism is the description of the change in the activation barrier with slowing the solvent relaxation at a given observation window of the experiment. Here, we focus on the reorganization energy. The way we approach the problem is to have the observation window set up by the length of simulations (1 ns) and to change the temperature of the solvent to observe how the reorganization energy defined by eq 3 falls out of ergodic behavior (eq 2) with lowering temperature. Once the transition to nonergodic behavior at fixed τ_{obs} is specified, this information can be funneled into eq 4 in order to calculate the reaction rates.[5]

* To whom correspondence should be addressed. E-mail: dmitrym@asu.edu.

10.1021/jp055235h CCC: $33.50
Published on Web 01/07/2006

We note that our simulation setup approaches the problem from the viewpoint of a single donor−acceptor complex. This situation is most relevant to natural photosynthesis in bacterial reaction centers and to single-molecule measurements of reaction rates which are becoming increasingly available.[9,10] Modeling of ET rates measured on ensembles of donor−acceptor complexes requires an additional input regarding the heterogeneous distribution of local environments,[11,12] which our current simulations do not provide.

As the second cumulant of the difference in the solute−solvent interaction potential (eqs 2 and 3), the solvent reorganization energy of ET is related to a response function of the solvent to the presence of the solute (see below). The latter can be related to a susceptibility of the pure solvent describing fluctuations of a nuclear collective coordinate coupled to the solute electronic states (dipolar polarization and density for dipolar solvents, quadrupolar polarization and density for nondipolar solvents).[13] Susceptibilities, which are second derivatives of a thermodynamic potential, are known to show specific behavior at points of thermodynamic instability (phase transitions) or at the onset of nonergodicity (glass transition). It is of general interest to understand how chemical reactions are affected by these special points.

For glass transitions, the heat capacity of a glassformer (the second cumulant of energy at constant volume or the second cumulant of entropy at constant pressure) passes through a peak which sharpens with increasing fragility of the liquid.[14] Here, we present simulation results indicating that the solvent reorganization energy of ET demonstrates a similar behavior. It first increases with lowering temperature and then sharply drops at the temperature of kinetic glass transition. The simulations have been done for a model charge-transfer complex (*p*-nitroaniline) in SPC/E water. This force-field solvent model has been extensively used to model dynamics and thermodynamics of low-temperature polar molecular liquids.[15−20] This model is therefore adopted here to study the statistics of solute−solvent interactions at low temperatures. We show that the arrested dynamics at the point of kinetic glass transition exhibits many qualitative features of molecular supercooled liquids observed in laboratory experiments. The results obtained here may therefore qualitatively apply to low-temperature ET kinetics even though they do not necessarily capture all the details of ET kinetics in aqueous solutions.

II. Simulation Results

We perform NVE and NPT molecular-dynamics (MD) simulations for a system composed of one solute (*p*-nitroaniline) and $N = 466$ water molecules, with periodic boundary conditions. All simulations are done for a cubic simulation cell with the side length $L = 24.075$ Å and the density of water 0.997 g/cm^3. The extended simple point charge model (SPC/E) is adopted for water. *p*-Nitroaniline is a small charge-transfer dye with a charge-transfer electronic transition resulting in about a 3.7 D change in the dipole moment.[21] The solute−solvent and solvent−solvent interactions are modeled by the sum of the long-range Coulombic potential and the short-range Lennard-Jones (LJ) potential. A spherical cutoff with the radius $L/2 = 12.0$ Å and Lorentz−Berthelot combination rules are used for the LJ interactions. The Coulombic interactions are treated by the Ewald summation method.[22] The Ewald method splits the sum over the periodic images of the simulation cell into a damped real space sum and a reciprocal space sum.[23] Summation in real space is truncated at $L/2$ (Ewald convergence parameter is 0.2346 Å^{-1}), and summation in reciprocal space involves approximately 2300 vectors with their magnitudes limited by 5.0 Å^{-1}. Simulations were done in the range of temperatures from supercooled region (50 K) to superheated region (509 K).[18−20,24] The length of simulations was 1.4 ns (400 ps equilibration) at $T > 220$ K and 6.8 ns (5.8 ns equilibration) at $T < 220$ K with a time step of 1 fs. The observation window for the calculation of λ_s was taken as 1 ns at the end of each simulation run.

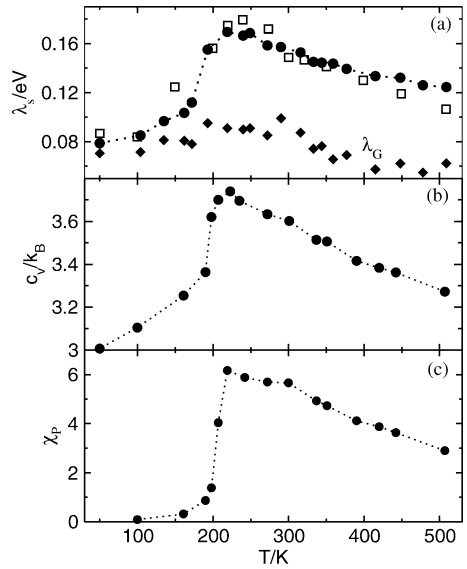

Figure 1. Reorganization energy (a), heat capacity (b), and dielectric susceptibility (c) vs T. In (a), circles refer to NVE simulations at $\rho = 0.997$ cm^3/g, squares indicate the NPT simulations at $P = 1$ atm, and diamonds refer to the fast Gaussian component of the solvent reorganization energy, λ_G. Dotted lines are drawn to guide the eye.

In parallel to solvation simulations, simulations of the pure SPC/E water ($N = 466$) at the same thermodynamic conditions have been done. For these simulations, equilibration was 400 ps long and production runs were 1.0 ns long at 220−509 K. At lower temperatures, the equilibration and production times were 800 ps and 6.0 ns, respectively. Configurations were stored at the intervals of 0.1 ps during the production runs. We have also obtained satisfactory energy and momentum conservation (energy fluctuation less than 1 in 10^5) throughout the production runs. Fluctuations of the average temperature were less than 5 K after equilibration of the system. Our simulations for pure SPC/E water are consistent with the results reported by Starr et al.[17] for 8000 SPC/E water molecules. They report −52.15 (3 ns equilibration) and −56.40 (4 ns equilibration) kJ/mol for the average interaction energy at 215 and 100 K, respectively. Our simulations give −51.68 and −56.10 kJ/mol at the same temperatures. The minor deviations may be attributed to slightly different densities, 1.0046 ($T = 245$ K) and 1.022 ($T = 100$ K) g/cm^3 in ref 17 compared to the constant density of 0.997 g/cm^3 in our simulations.

Atomic charges of *p*-nitroaniline were obtained by fitting the electrostatic potential from ab initio electron structure calculations using GAUSSIAN'03.[25] The ground-state geometry of *p*-nitroaniline was obtained on the MP2 level (6-31+G*) using X-ray data[26] for the initial geometry. The excited-state charge distribution is obtained from CIS calculations. The ground, 7.18 D, and excited, 10.88 D, dipoles are in reasonable agreement with the literature data.[21,27] Coordinates and charges of *p*-nitroaniline in the ground and excited states are given in the Supporting Information.

Figure 1a shows the solvent reorganization energy calculated according to eq 3 in which the energy gap ΔE is replaced with

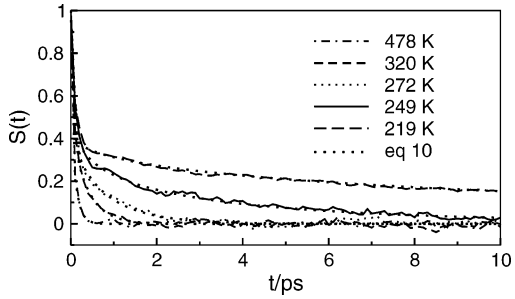

Figure 2. Stokes shift correlation function (eq 7) of ground-state *p*-nitroaniline in SPC/E water.

the difference of the solute−solvent interaction potential in the charge-transfer (S_4) and ground (S_0) electronic states.[21] The average is performed over the simulation trajectories generated for the solute in the ground state. The circles indicate constant-volume simulations, and the squares refer to simulations at a constant pressure of $P = 1$ atm. The reorganization energy increases with lowering temperature in the high-temperature liquid[13] and then turns down and drops sharply at $T^* \simeq 219$ K.

Shown in parts b and c of Figure 1 are also the heat capacity

$$c_V/k_B = {}^3/_2 + \langle(\delta E)^2\rangle_{obs}/N(k_BT)^2 \qquad (5)$$

and dielectric susceptibility

$$\chi_P = (k_BTV)^{-1}\langle(\delta \mathbf{M})^2\rangle_{obs} \qquad (6)$$

of SPC/E water (E is the total energy and $\mathbf{M}$ is the total dipole moment of a sample of liquid with volume V containing N molecules). Both solvent susceptibilities show the dependence on temperature very similar to that of λ_s. Figure 1 thus stresses the similarity in the temperature variation of the ET reorganization energy and susceptibilities of the pure solvent at the onset of nonergodicity at $T = T^*$.

The decay of c_V and χ_P at T^* should be understood as a kinetic transition occurring at the crossing of the relaxation times given by the peaks of $c_V''(\omega)$ and $\chi_P''(\omega)$ with the observation time of the simulation experiment (a few nanoseconds). Similarly, the dip in the reorganization free energy is related to the crossing of the slow relaxation time of the Stokes shift dynamics with the observation time of the computer experiment. When the equilibrium Stokes shift correlation function[28] (Figure 2)

$$S(t) = C(t)/C(0), \quad C(t) = \langle\delta\Delta E(t)\delta\Delta E(0)\rangle \qquad (7)$$

is available, the effect of the finite observation window can be understood by imposing a stepwise cutoff on frequencies below $\omega_{obs} = 2\pi/\tau_{obs}$. The equilibrium reorganization energy λ_0 in eq 2 is then given by the full integral over all frequencies of the imaginary part of the Stokes shift response function[29] $\chi''(\omega) = (\pi\omega/k_BT)C(\omega)$, where $C(\omega)$ is the frequency Fourier transform of $C(t)$

$$\lambda_0 = \int_0^\infty \chi''(\omega)(d\omega/\pi\omega) \qquad (8)$$

Correspondingly, the nonergodic reorganization energy is obtained by limiting the range of frequencies to those higher than ω_{obs}

$$\lambda_s = \int_{\omega_{obs}}^\infty \chi''(\omega)(d\omega/\pi\omega) \qquad (9)$$

Equation 8 indeed describes the simulations well[30] once the fully equilibrated response function $\chi''(\omega)$ can be obtained from MD simulations. This function is not available below T^* since our data on the Stokes shift dynamics are limited to $T > T^*$.

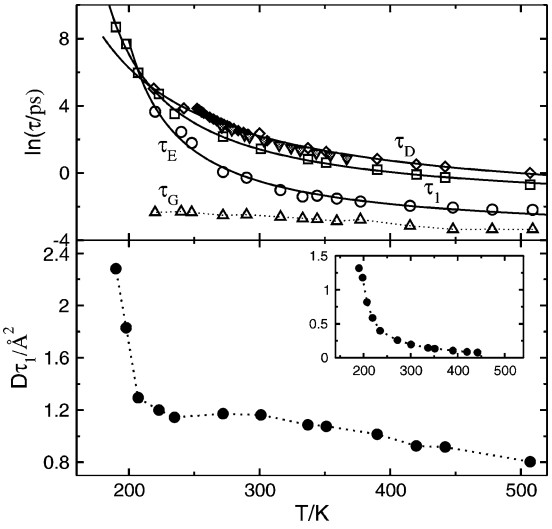

Figure 3. Upper panel: relaxation times τ_G, τ_E (solvation dynamics, eq 10), τ_1 (one-particle orientational relaxation, eq 11), and τ_D (Debye dielectric relaxation) vs T. The solid lines indicate the VF fits. The closed diamonds refer to the experimental dielectric relaxation of supercooled water (constant pressure),[32] while the half-open triangles refer to the data from ref 33. Lower panel: the product of the self-diffusion coefficient and the rotational relaxation time τ_1 vs T. The inset shows the maximum value $\alpha_2(t^*)$ of the non-Gaussian parameter $\alpha_2(t)$ defined by eq 13.

The reorganization energy does not drop to zero but instead levels off at low temperatures. The low-temperature component of λ_s is related to fast phonon-like solvent modes which do not become dynamically arrested below T^*. The fast reorganization component is clearly seen as the initial Gaussian decay of $S(t)$ fitted to a biphasic form containing the Gaussian (G) and stretched exponential (E) parts

$$S(t) = A_G e^{-(t/\tau_G)^2} + (1 - A_G)e^{-(t/\tau_E)^\beta}. \qquad (10)$$

The stretching exponent β obtained from the fit is equal to one above 272 K and starts to drop below this temperature reaching the value of 0.34 at 219 K (see Supporting Information). From the fit of the simulated Stokes shift data, the Gaussian relaxation time[28] $\tau_G \simeq 70$ fs is weakly temperature dependent and is approximately given by a linear function of T (K): $\ln(\tau_G(T)/\text{ps}) = -1.34 - 0.0042 \times T$, $220 < T < 509$ K (Figure 3). In contrast, the exponential relaxation time τ_E increases sharply with lowering T values and can be approximated by the Vogel−Fulcher (VF) law: $\ln(\tau_E(T)/\text{ps}) = -3.73 + 447/(T - 161)$, $220 < T < 509$ K.[31] The Gaussian reorganization component, $\lambda_G = A_G\lambda_0$, turns out to be weakly dependent on temperature (Figure 1a, diamonds). The combination of weak temperature dependence of λ_G with ultrafast relaxation of the Gaussian component of $S(t)$ clearly indicates that it is the slow exponential component of $S(t)$ that becomes dynamically arrested at the transition to nonergodicity. The drop of λ_s at $T < T^*$ is thus equal to $\lambda_E = (1 - A_G)\lambda_0$. Despite long equilibration, water at the lowest temperatures studied here may still not be fully equilibrated. This has, however, only a minor effect on λ_s since it is affected only by fast, phonon-like relaxation at low temperatures.

The slow component of the Stokes shift dynamics can be identified with collective orientational relaxation of the dipolar polarization of water related to the frequency-dependent dielectric constant $\epsilon(\omega)$, which was obtained from simulations according to the formalism described in refs 34 and 35. The

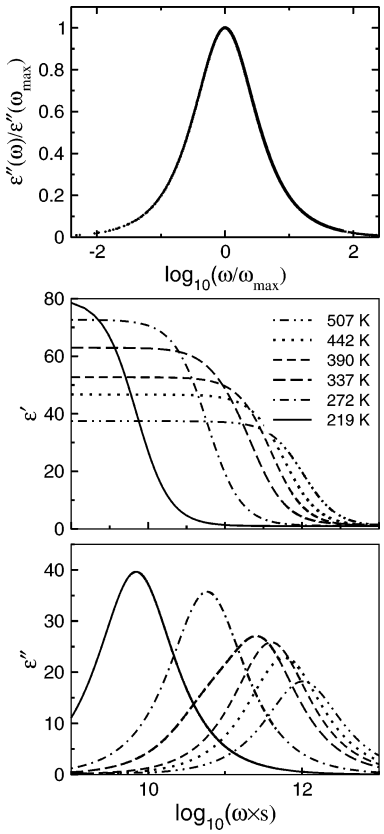

Figure 4. Real ($\epsilon'(\omega)$) and imaginary ($\epsilon''(\omega)$) parts of the frequency-dependent dielectric constant of SPC/E water at different temperatures. The upper panel shows the rescaled dielectric loss $\epsilon''(\omega)/\epsilon(\omega_{max})$ vs $\log(\omega/\omega_{max})$ calculated at 198, 219, 242, and 300 K; ω_{max} is the frequency maximum of the dielectric loss function. The data points at different temperatures cannot be distinguished on the plot scale.

variation of $\epsilon(\omega)$ with lowering temperature (Figure 4) is characteristic of many polar glassformers[36,37] and supercooled water.[32,38] In particular, the peak ω_{max} of the dielectric loss $\epsilon''(\omega)$ shifts to lower frequencies with cooling the solvent. The corresponding Debye relaxation time, $\tau_D = 1/\omega_{max}$ (diamonds in Figure 3), compares very well to the experimentally reported values[32,33] (closed diamonds and half-open triangles in Figure 3). A similarly good agreement was reported previously by Rønne et al.[33] for MD simulations in a narrower temperature range ($271.5 \le T \le 368.15$) on a smaller system (216 SPC/E molecules, 4 ns runs with the time step of 2 fs). We still need to mention the approximate nature of the water model used in simulations, in particular the fact that the SPC/E force field does not include molecular polarizability.

The width of the dielectric spectrum does not change with changing temperature, and the dielectric loss data at different temperatures can be superimposed on one master curve by proper rescaling (Figure 4, upper panel). The increase in the width of dielectric loss is commonly associated with liquid heterogeneity.[36,39,40] The Debye dielectric loss shown in Figure 4 thus indicates that the dielectric response is homogeneous.

The collective relaxation of solvation shells reflected by $\tau_E(T)$ can be compared to the single-particle correlation function of the dipole vector $\mathbf{m}(t)$

$$C_1(t) = \langle \mathbf{m}(t)\cdot\mathbf{m}(0)\rangle/\langle \mathbf{m}(0)^2\rangle \qquad (11)$$

The relaxation time $\tau_1(T)$ for $C_1(t)$ shows a super-Arrhenius[41] temperature dependence (Figure 3) which can be approximated by the VF law: $\ln(\tau_1(T)/\text{ps}) = -2.15 + 578/(T - 137)$. Our

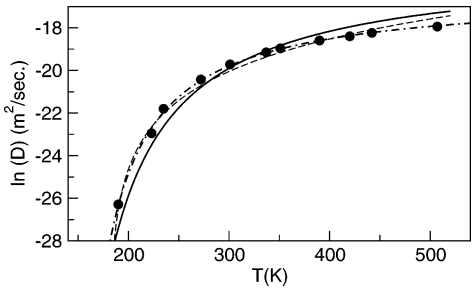

Figure 5. Diffusion coefficient of SPC/E water from current simulations (points) compared with experimental self-diffusivity of supercooled water (solid line) given by the VF fit: $\ln(D \times \text{s/m}^2) = -15 - 892/(T - 118)$.[45] The dashed and dash−dotted lines refer to the power-law and VF fits of the simulation data, respectively.

results for $\tau_1(T)$ are consistent with earlier reports by Sciortino et al.[16] for 216 SPC/E water molecules (see Supporting Information). The Debye relaxation time $\tau_D(T)$ is somewhat higher than $\tau_1(T)$ with the VF fit: $\ln(\tau_D(T)/\text{ps}) = -2.35 + 961/(T - 88.2)$.

What is the nature of the dynamical arrest occurring below ≃219 K? Previous extensive simulations of SPC/E water have shown a power-law temperature dependence of transport coefficients with the critical temperature of ca. $T_c \simeq 186-200$ K.[15,16,42,43] On the basis of this observation and scaling laws for the intermediate scattering function, the critical temperature was assigned to the ideal ergodic-to-nonergodic kinetic glass transition predicted by the mode-coupling theory (MCT).[44] Our data for the self-diffusion coefficient $D(T)$ of SPC/E water (obtained from MD trajectories using the Einstein relation) embrace a broader range of temperatures than those reported in refs 15 and 16. The self-diffusion coefficient (Figure 5) can be fitted by both the power-law ($\ln(D(T) \times \text{s/m}^2) = -19 + 2.5\ln(T/181 - 1)$) and VF ($\ln(D(T) \times \text{s/m}^2) = -16.5 + 540/(T - 136)$) functions, with the latter providing a better global fit. The diffusivity data from simulations compare favorably with experimental self-diffusivity of supercooled water reported in ref 45 (Figure 5). The power law has been previously reported to give poor fits for temperatures below the MCT T_c,[46−49] while the VF formula sometimes fails at $T > T_c$ where the power law applies.[50] The limiting VF temperatures for single-particle correlations reflected by $D(T)$ and $C_1(T)$ (136 and 137 K, respectively) are significantly lower than the corresponding temperature (161 K) from the many-particle correlation time $\tau_E(T)$.[31]

The temperature T^* at which $\lambda_s(T)$ and solvent susceptibilities start to drop also marks the onset of the separation of translational and rotational diffusion signaling the breakdown of the Stokes−Einstein relation (Figure 3, lower panel)[50−52]

$$D(T) \times \tau_1(T) \simeq \text{const} \qquad (12)$$

Indeed, the product of the diffusion coefficient and the rotational relaxation time is approximately constant down to the temperature $T_c \simeq 207$ K.[53] If 165 K is adopted as the glass transition temperature for water,[31] then the onset of translational enhancement falls in the range of $1.2-1.3T_g$ found in laboratory experiment.[51] Apart from the MCT critical temperature, the separation of diffusivity and rotational relaxation can be related to the crossover temperature of Rössler scaling,[54] the bifurcation of the α- and β-relaxation,[52] and the Stickel T_B temperature.[49]

The rise of $D\tau_1$ is commonly explained by either static spatial[55−58] or dynamic[59] heterogeneity. In the frustration-limited domain picture of Tarjus and Kivelson,[55,56] the turning temperatures in Figures 1 and 3 can be associated with the onset of

domain formation. This interpretation is questionable, however, given the small size of our simulation box which cannot incorporate mesoscopic domains. Note also that no discontinuous change in pair distribution functions is seen at T^* except commonly observed[16,60] sharpening of solvation shell peaks.

The results of our simulations better fit the picture of spatially heterogeneous dynamics which assumes the presence in a supercooled liquid of groups of mobile molecules.[59,61,62] These groups may represent clusters of hydrogen bond defects in SPC/E water,[62] chains of mobile particles in monatomic LJ fluids,[61] or some other structures. The collective motion of such mobile heterogeneities provides the enhancement of translational diffusion which is correlated with the increase of the non-Gaussian parameter[60−62]

$$\alpha_2(t) = 3\langle r^4(t)\rangle/5\langle r^2(t)\rangle^2 - 1 \qquad (13)$$

where $\langle r^2(t)\rangle$ is the mean-square displacement. The maximum value $\alpha_2(t^*)$ (Figure 3, lower panel inset) is reached at time t^*. Both $\alpha_2(t^*)$ and t^* grow with cooling indicating increasing dynamic heterogeneity of molecular translations. On the other hand, dielectric loss data (Figure 4) show no heterogeneity suggesting a more homogeneous distribution of molecular rotations.

This interpretation is consistent with recent dielectric data by Richert et al.[63,64] which do not show any increase in spatial heterogeneity in the region of temperatures $T_g \le T \le 1.2T_g$ where previous reports[58] had indicated the breakdown of the Stokes−Einstein relation. Although no broadly accepted explanation of this phenomenon currently exists, the onset of translation/rotation decoupling is normally associated with the critical MCT temperature.[50,52] We will therefore resort to the interpretation of temperature T^* at which λ_s dips to its Gaussian component as the point of kinetic transition to nonergodicity with many features of the critical temperature of an ideal glass transition predicted by MCT.[44]

The mechanism reported here may be relevant to ET in proteins. The Debye−Waller factor of proteins starts to rise sharply at a temperature close to T_c indicating an increased conformational mobility of the protein matrix and its hydration shell.[65] Our present analysis then suggests a sharp rise of the corresponding reorganization energy at that temperature.

III. Concluding Remarks

The MCT critical temperature T_c located above the calorimetric glass transition temperature marks the change in the mechanism of relaxation in viscous liquids. Above T_c, transport phenomena and response to a solute field are dominated by the rattling and librations of particles in self-consistently maintained cages. Below T_c, on the other hand, the particles are almost arrested in the free-energy landscape and transport and relaxation are triggered by thermally activated hopping and rotation over saddle points. The hopping mechanism is recorded by experiments with the observation window up to 10^2 s in the temperature range $T_g \le T \le T_c$. Many redox reactions occur on the nanosecond and faster time scale. Since hopping relaxation does not occur on the reaction time scale, MCT formalism may appear to be appropriate for describing ET reactions in viscous supercooled liquids. The sharp drop of the solvent reorganization energy close to $T^* \simeq T_c$ found in our simulations is therefore expected to mimic the laboratory ET experiment.

The modeling of ET kinetics in the nonergodic regime, when transition-state description fails, requires the knowledge of how the solvation energetics, represented here by the solvent reorganization energy, change with slowing down solvent relaxation or, alternatively, narrowing the observation window. The formal modeling of this effect may be achieved by applying the ideas developed in MCT with a possibility of deriving the frequency filter required to model nonergodic reorganization energy (eq 9) and the activation barrier.

Acknowledgment. This research was supported by the National Science Foundation (CHE-0304694). This is publication #643 from the ASU Photosynthesis Center. Useful discussions with Prof. C. A. Angell and Prof. R. Richert are gratefully acknowledged.

Supporting Information Available: (1) Atomic coordinates and ground/excited charges of *p*-nitroaniline, (2) fitting parameters for the Stokes shift correlation function, and (3) plots of mean-squared deviations in SPC/E water at different temperatures. This material is available free of charge via the Internet at http://pubs.acs.org.

References and Notes

(1) Marcus, R. A. *Rev. Mod. Phys.* **1993**, *65*, 599.
(2) Gardiner, C. W. *Handbook of stochastic methods*; Springer: Berlin, 1997.
(3) Grote, R. F.; Hynes, J. T. *J. Chem. Phys.* **1980**, *73*, 2715.
(4) Barzykin, A. V.; Frantsuzov, P. A.; Seki, K.; Tachiya, M. *Adv. Chem. Phys.* **2002**, *123*, 511.
(5) Matyushov, D. V. *J. Chem. Phys.* **2005**, *122*, 084507.
(6) Dick, L. A.; Malfant, I.; Kuila, D.; Nebolsky, S.; Nocek, J. M.; Hoffman, B. M.; Ratner, M. A. *J. Am. Chem. Soc.* **1998**, *120*, 11401.
(7) Frauenfelder, H.; Parak, F.; Young, R. D. *Annu. Rev. Biophys. Biophys. Chem.* **1998**, *17*, 451.
(8) Andreatta, D.; Pérez, J. L.; Kovalenko, S. A.; Ernsting, N. P.; Murphy, C. J.; Coleman, R. S.; Berg, M. A. *J. Am. Chem. Soc.* **2005**, *127*, 7270.
(9) Lu, H. P.; Xie, X. S. *J. Phys. Chem. B* **1997**, *101*, 2753.
(10) Holman, M. W.; Liu, R.; Adams, D. M. J. *Am. Chem. Soc.* **2003**, *125*, 12649.
(11) Marcus, R. A. *J. Phys. Chem.* **1990**, *94*, 4963.
(12) Rhodes, T. A.; Farid, S.; Goodman, J. L.; Gould, I. R.; Young, R. H. *J. Am. Chem. Soc.* **1999**, *121*, 5340.
(13) Matyushov, D. V. *J. Chem. Phys.* **2004**, *120*, 7532.
(14) Angell, C. A. *Science* **1995**, *267*, 1924.
(15) Gallo, P.; Sciortino, F.; Tartaglia, P.; Chen, S.-H. *Phys. Rev. Lett.* **1996**, *76*, 2730.
(16) Sciortino, F.; Gallo, P.; Tartaglia, P.; Chen, S.-H. *Phys. Rev. E* **1996**, *54*, 6331.
(17) Starr, F. W.; Bellissent-Funel, M.-C.; Stanley, H. E. *Phys. Rev. E* **1999**, *60*, 1084.
(18) Stanley, H. E.; Buldyrev, S. V.; Canpolat, M.; Mishima, O.; Sadr-Lahijany, M. R.; Scala, A.; Starr, F. W. *Phys. Chem. Chem. Phys.* **2000**, *2*, 1551.
(19) Debenedetti, P. G.; Stanley, H. E. *Phys. Today* **2003**, *56*, 40.
(20) Giovambattista, N.; Angell, C. A.; Sciortino, F.; Stanley, H. E. *Phys. Rev. Lett.* **2004**, *93*, 047801.
(21) Farztdinov, V. M.; Schanz, R.; Kovalenko, S. A.; Ernsting, N. P. *J. Phys. Chem. A* **2000**, *104*, 11486.
(22) DeLeeuw, S. W.; Perram, J. W.; Smith, E. R. *Proc. R. Soc. London, Ser. A* **1980**, *373*, 27.
(23) Smith, W.; Forester, T. R. *J. Mol. Graphics* **1996**, *14*, 136−141.
(24) Vega, C.; Sanz, E.; Abascal, J. L. F. *J. Chem. Phys.* **2005**, *122*, 114507.
(25) Frisch, M. J.; Trucks, G. W.; Scuseria, G. E.; Robb, M. A.; Cheeseman, J. R.; Zakrzewski, V. G. *GAUSSIAN 03*; Gaussian, Inc.: Pittsburgh, PA, 2003.
(26) Donohue, J. *Acta Crystallogr.* **1956**, *9*, 960.
(27) Rashid, A. N. *J. Mol. Struct.* **2004**, *681*, 57.
(28) Jimenez, R.; Fleming, G. R.; Kumar, P. V.; Maroncelli, M. *Nature* **1994**, *369*, 471.
(29) Hansen, J. P.; McDonald, I. R. *Theory of Simple Liquids*; Academic Press: New York, 2003.
(30) Ghorai, P. K.; Matyushov, D. V. *J. Am. Chem. Soc.* **2006**, *127*, 16390.
(31) The Vogel−Fulcher temperature for $\tau_E(T)$ falls slightly below $T_g \simeq 165$ K recently identified as the glass transition temperature of water; see Yue, Y.-Z.; Angell, C. A. *Nature* (London) **2004**, *427*, 717 and *Nature*

(London) **2005**, *435*, E1. The assignment of T_g of water is still controversial; see Johari, G. P. *J. Chem. Phys*. **2002**, *116*, 8067.

(32) Bertolini, D.; Cassettari, M.; Salvetti, G. *J. Chem. Phys*. **1982**, *76*, 3285.

(33) Rønne, C.; Thrane, L.; Åstrand, P.-O.; Walqvist, A.; Mikkelsen, K. V.; Keiding, S. R. *J. Chem. Phys*. **1997**, *107*, 5319.

(34) Neumann, M. *Mol. Phys*. **1986**, *57*, 97.

(35) Omelyan, I. P. *Mol. Phys*. **1998**, *93*, 123.

(36) Dixon, P. K.; Wu, L.; Nagel, S. R.; Williams, B. D.; Carini, J. P. *Phys. Rev. Lett*. **1990**, *65*, 1108.

(37) Schneider, U.; Lunkenheimer, P.; Brand, R.; Loidl, A. *J. Non-Cryst. Solids* **1998**, *235*−*237*, 173.

(38) Johari, G. P. *Phys. Chem. Chem. Phys*. **2000**, *2*, 1567.

(39) Ediger, M. D. *Annu. Rev. Phys. Chem*. **2000**, *51*, 99.

(40) Richert, R. J. *Phys*.: *Condens. Matter* **2002**, *14*, R703.

(41) Garrahan, J. P.; Chandler, D. *Proc. Natl. Acad. Sci. U.S.A.* **2003**, *100*, 9710.

(42) Fabbian, L.; Latz, A.; Schilling, R.; Sciortino, F.; Tartaglia, P.; Theis, C. *Phys. Rev. E* **1999**, *60*, 5768.

(43) Theis, C.; Sciortino, F.; Latz, A.; Schilling, R.; Tartaglia, P. *Phys. Rev. E* **2000**, *62*, 1856.

(44) Götze, W. Aspects of structural glass transitions. In *Liquids, freezing and glass transition*; Hansen, J. P., Levesque, D., Zinn-Justin, J., Eds.; Elsevier: Amsterdam, The Netherlands, 1991; Vol. 1.

(45) Smith, R. S.; Kay, B. D. *Nature* **1999**, *398*, 788.

(46) Angell, C. A. *Annu. Rev. Phys. Chem*. **1983**, *34*, 593.

(47) Taboreck, P.; Kleiman, R. N.; Bishop, D. J. *Phys. Rev. B* **1986**, *34*, 1835.

(48) Murthy, S. S. N. *J. Mol. Liq*. **1990**, *44*, 211.

(49) Stickel, F.; Fischer, E. W.; Richert, R. *J. Chem. Phys*. **1995**, *102*, 6251.

(50) Rössler, E. *J. Non-Cryst. Solids* **1991**, *131*−*133*, 242.

(51) Chang, I.; Sillescu, H. *J. Phys. Chem. B* **1997**, *101*, 8794.

(52) Ediger, M. D.; Angell, C. A.; Nagel, S. R. *J. Phys. Chem*. **1996**, *100*, 13200.

(53) The temperature $T_c = 207$ K from the plot of $D(T)\tau_1(T)$ vs T is very close to the estimate for the critical temperature $T_c \simeq 208$ K from the molecular MCT with a restricted set of correlation functions (dipole approximation).[42] This agreement is, however, fortuitous since the full version of the molecular MCT leads to a substantially higher temperature, $T_c \simeq 279$ K.[43]

(54) Rössler, E.; Hess, K.-U.; Novikov, V. N. *J. Non-Cryst. Solids* **1998**, *223*, 207.

(55) Tarjus, G.; Kivelson, D. *J. Chem. Phys*. **1995**, *103*, 3071.

(56) Kivelson, D.; Tarjus, G. *Philos. Mag. B* **1998**, *77*, 245.

(57) Xia, X.; Wolynes, P. G. *J. Phys. Chem. B* **2001**, *105*, 6570.

(58) Swallen, S. F.; Bonvallet, P. A.; McMahon, R. J.; Ediger, M. D. *Phys. Rev. Lett*. **2003**, *90*, 015901.

(59) Jung, Y. J.; Garrahan, J. P.; Chandler, D. *Phys. Rev. E* **2004**, *69*, 061205.

(60) Donati, C.; Glotzer, S. C.; Poole, P. H.; Kob, W.; Plimpton, S. J. *Phys. Rev. E* **1999**, *60*, 3107.

(61) Schober, H. R. *Phys. Chem. Chem. Phys*. **2004**, *6*, 3654.

(62) Giovambattista, N.; Mazza, M. G.; Buldyrev, S. V.; Starr, F. W.; Stanley, H. E. *J. Phys. Chem. B* **2004**, *108*, 6655.

(63) Richert, R.; Duvvuri, K.; Duong, L.-T. *J. Chem. Phys*. **2003**, *118*, 1828.

(64) Richert, R. *J. Chem. Phys*. **2006**, *123*, 154502.

(65) Bizzarri, A. R. *J. Phys*.: *Condens. Matter* **2004**, *16*, R83.